Available online at www.sciencedirect.com
SCIENCE DIRECT®
Journal of Photochemistry and Photobiology A: Chemistry 163 (2004) 61–67
Journal of Photochemistry and Photobiology A:Chemistry
www.elsevier.com/locate/jphotochem

Photophysical properties of an extended bis-oxonol dye

Andrew C. Benniston*, Anthony Harriman[1], Iain E. McCulloch, Maryam Mehrabi, Sarah A. Rostron, Craig A. Sams

Molecular Photonics Laboratory, School of Natural Sciences (Chemistry), University of Newcastle, Bedson Building, Newcastle upon Tyne NE1 7RU, UK

Received 8 July 2003; received in revised form 8 July 2003; accepted 31 October 2003

Abstract

A bis-oxonol dye has been prepared from reaction between *N*,*N*′-dibutylthiobarbituric acid and glutacondialdehyde dianil monohydrochloride. The dye comprises two *N*,*N*′-dibutylthiobarbiturate units connected via a pentamethine spacer, and detailed ^{1}H NMR (2D-COSY, NOESY) experiments confirm that the polyene backbone is in the all-*trans* arrangement. The dye is intensely blue in colour, absorbing around 640 nm in ethanol with a molar absorption coefficient of 175,000 mol^{-1} dm^3 cm^{-1}. Under illumination, the first-excited all-*trans* singlet state is formed but suprisingly there is little or no isomerisation to a *cis* isomer. Quantum chemical calculations suggest that there is a high barrier to isomerisation in the ground state while the absence of photoisomerisation is attributed to ineffective population of the relevant LUMO at the S_1 level. The dye, which possesses an unusually long-lived singlet excited state for a cyanine-type dye, shows modest capacity for transporting potassium cations across a membrane and functions as an excellent acceptor for electronic energy transfer from other cyanine dyes.

Keywords: Oxonol dye; Fluorescence; Membrane; Ion transport

1. Introduction

Current interest in cyanine dyes can be traced to their attractive photophysical properties, and resultant beneficial uses in such areas as photodynamic therapy [1] and fluorescent probes for monitoring the concentrations of intracellular species [2]. Often this type of dye is used to procure information about membrane fluidity, viscosity, polarity, potential and phase-transition temperature [3]. As part of our own research effort, the dynamics of light-induced and thermal isomerisation of cyanine derivatives [4], such as the bis-oxonol (OXO), have been studied extensively. This latter dye has found limited use in the coulometric analysis of liperoxides formed by in situ oxidation of lipid membranes [5] and for fluorometric determination of membrane potentials [6]. The chromophore unfortunately has been shown to undergo photoisomerisation from the first-excited singlet state on the time scale of a few tens of picoseconds. The resultant isomer reverts to the original configuration over several microseconds. Our earlier studies were able to rationalise the thermal isomerisation process in terms of the rotor volume and viscosity effects [7]. As well as light-induced isomerisation, a further drawback of OXO is its absorption/fluorescence profile which being located at ca. 570 nm is not ideal for use in biological environments. Dyes that absorb and emit in the red spectral region are highly prized in the biomedical field [8].

Herein, we report the properties of a bis-oxonol dye (OXON) which contains a more extended polymethine backbone, and hence absorbs and fluoresces well into the red end of the visible spectral region. This dye has warranted commercial exploitation for detection of membrane potentials using fluorescence energy-transfer methods [9]. Even so, scant attention has been paid to the photophysical behaviour of this dye. We have now carried out a detailed examination of the fluorescence properties of OXON in different solvents and compared the derived values to those determined earlier for OXO under the same conditions. To our surprise, the two dyes show markedly different photophysical properties despite the close similarity of their structures.

2. Experimental

Starting materials were purchased from Aldrich and were used as received. Potassium picrate (CARE!) was prepared by careful neutralisation of a solution of picric acid with

* Corresponding author. Tel.: +44-191-222-5706; fax: +44-191-222-6929.
E-mail address: a.c.benniston@ncl.ac.uk (A.C. Benniston).
[1] Co-corresponding author.

1010-6030/$ – see front matter © 2004 Elsevier B.V. All rights reserved.
doi:10.1016/S1010-6030(03)00433-7

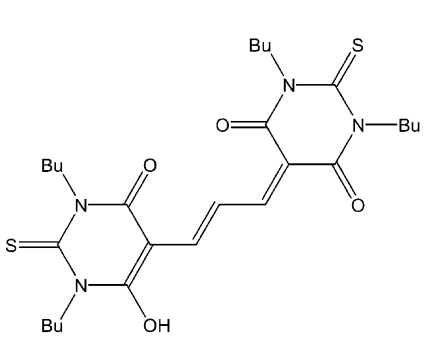

OXO

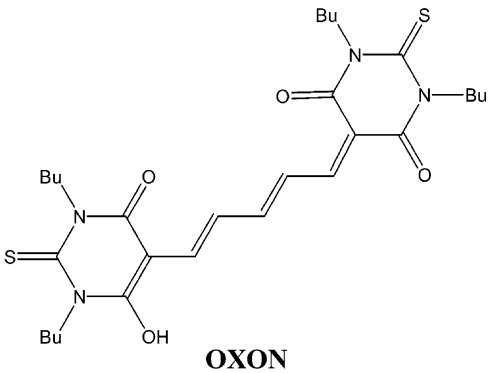

OXON

K_2CO_3. Solvents were dried according to standard literature procedures. ^{1}H NMR spectra were obtained using a Jeol Lambda500 500 MHz spectrometer using the solvent as internal standard. Mass spectra were recorded using the EPSRC mass spectrometry service at Swansea. Detailed molecular modelling calculations were performed using the commercial package AMPAC at the AM1 semi-empirical level. The effect of solvent was treated using the COSMO module. Transport experiments using potassium picrate were carried out with a membrane solvent (1-decanol) immobilised in a porous polymeric filter. The filter was sealed in a teflon holder and positioned vertically between two compartments of a cell containing, on one side, potassium picrate and, on the other side, the receiving phase of citric acid. The extent of potassium ion transport across the membrane was measured by monitoring the appearance of the picrate ion (358 nm, $\varepsilon_{max} = 14,500\,mol^{-1}\,dm^3\,cm^{-1}$) [10] in the receiving phase by UV-visible spectroscopy. Blank experiments were run with one or more of the ingredients being omitted from the system. Absorption spectra were recorded with a Hitachi U3310 spectrophotometer and fluorescence spectra were recorded with a fully-corrected Hitachi F4500 spectrofluorimeter. All emission studies were made using optically dilute solutions at 20 °C unless stated otherwise. Fluorescence quantum yields were measured relative to free-base meso-tetraphenylporphyrin in toluene [11]. The fluorescence lifetimes were measured with a Spex Fluorolog tau-3 fluorescence spectrometer using optically dilute samples, after deconvolution of the instrument response function.

2.1. Preparation of OXON

1,3-Dibutyl-2-thiobarbituric acid (200 mg, 0.59 mmol) and glutacondialdehyde dianil monohydrochloride (84 mg, 0.295 mmol) were mixed in dry pyridine (1 ml) and stirred for 2 h. The pyridine was removed on a rotary evaporator and the crude material purified by medium-pressure column chromatography (silica gel), eluting first with $CHCl_3$ to remove impurities and then with $CHCl_3$:MeOH (9:1) to obtain the desired product. Yield 62 mg, 37%. ^{1}H NMR (d_4-MeOD) δ = 0.86–0.89 (t, 12H, J = 7.4 Hz, CH_3–CH_2), 1.19–1.32 (m, 8H, CH_3–CH_2–CH_2), 1.59 (m, 8H, N-$CH_2CH_2CH_2$), 4.34–4.38 (m, 8H, N-CH_2–CH_2), 7.46–7.49 (t, 1H, J = 12.3 Hz, CH_c), 7.68–7.75 (dd, 2H, J = 12.9 Hz, J' = 12.2 Hz, CH_b), 7.79–7.83 (d, 2H, J = 13.7 Hz, CH_a). FAB-MS (NBA matrix) m/z = 574 (MH^+). IR (KBr disc) 3417 (OH), 2958, 2930, 2870 (CH), 1618 (C=O). UV-visible (EtOH) λ (nm)) ε_{max} ($mol^{-1}\,dm^3\,cm^{-1}$) = 638 (175,000). Elemental analysis calc. (found) for $C_{29}H_{42}N_4O_4S_2{\cdot}4H_2O$; C, 53.85 (53.73); H, 7.79 (7.13); N, 8.66 (8.45).

3. Results and discussion

3.1. Structure of the ground state

The authenticity of OXON was established by ^{1}H NMR COSY and NOESY spectra, as well as exact-mass spectrometry. Inspection of a computer generated space-filling model of the dye supported an all-*trans* arrangement of the protons in the polyene backbone in preference to a *cis* isomer which suffered from severe steric crowding. This hypothesis was fully supported by high-resolution ^{1}H NMR spectroscopy carried out in d_4-MeOD solution (Fig. 1).

Thus, examination of the coupling constants observed for the pentamethine protons, which are unequivocally identified by their chemical shifts, permits total assignment of the ground-state structure. Hence, the ^{1}H NMR spectrum shows a doublet (corresponding to two protons), a doublet of a doublet (corresponding to two protons) and a triplet (corresponding to one proton) at 7.83, 7.72 and 7.46 ppm, respectively. The doublet at 7.83 ppm can be readily assigned to protons Ha,Ha′ which display a direct correlation to the resonance centred at 7.72 pmm which, therefore, can be assigned to protons Hb,Hb′. The direct correlation between this resonance and that centred at 7.46 ppm confirms the proton assignment. The coupling constants fall within the range of 12.2–13.7 Hz and are consistent with either an all-*cis* or all-*trans* configuration of the pentamethine protons. Complete verification of the structure was made by inspection of the correlated peaks in a NOESY spectrum of the dye in d_4-MeOD (Fig. 2). As required for the all-*trans* arrangement, there are distinct NOEs between proton Hc

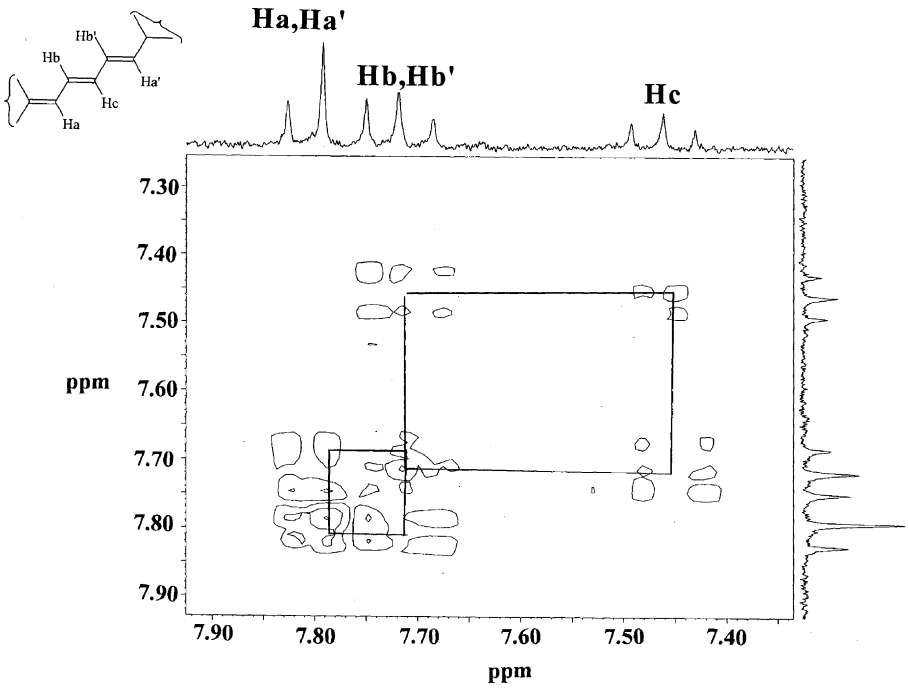

Fig. 1. Partial 500 MHz ^{1}H NMR COSY spectrum of OXON in d_4-MeOD.

and the two protons Ha,Ha′ as well as between Hc and the two protons Hb,Hb′.

The FTIR spectrum of OXON (KBr disc) also showed the absence of extensive intramolecular H-bonding between terminal methine protons and the C=O groups of the barbiturate unit. The carbonyl region contained only one signal at 1618 cm^{-1}. This behaviour is different to the intramolecular interactions shown to exist in the shorter OXO and in related cyanine dyes [12]. It is also worth noting that the C–N amide bonds retain some double bond character, which effectively brings the terminal C=S bond into partial conjugation with the rest of the molecule.

3.2. Molecular modelling

A set of quantum chemical calculations was made in order to assess likely ground-state conformations and possible sites for light-induced isomerisation of the compound.

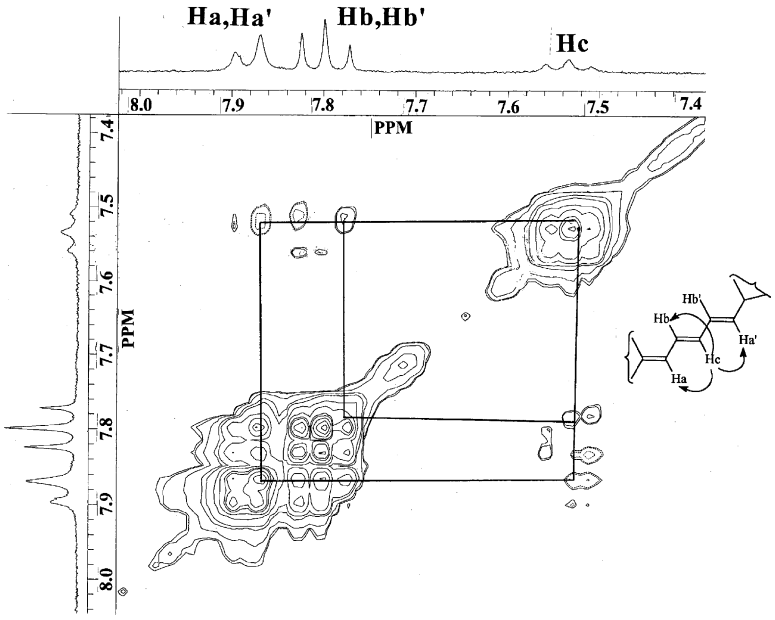

Fig. 2. Partial 500 MHz ^{1}H NMR NOESY spectrum of OXON in d_4-MeOD.

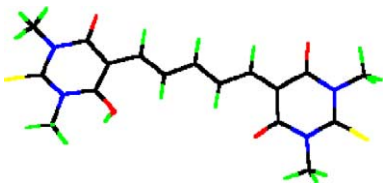

Fig. 3. Computer generated ball and stick representation of one of the all-*trans* isomers of OXON.

The calculations were made by means of the semi-empirical Hartree-Foch Austin Model 1 (AM1) method at the CAS-CI level. A total of five unoccupied and five occupied MOs were used for all calculations and the influence of solvent was taken into account using the COSMO module available in AMPAC. All computations were made with AMPAC. The periodic boundary condition was applied with a solvent box $36 \times 48 \times 48\,\text{Å}^3$ filled with water molecules.

The lowest-energy conformation was computed at the AM1 level to have the pentamethine chain arranged in an all-*trans* configuration but with the double bond localised on the barbiturate unit held in a *cis* arrangement with the nearest double bond of the polymethine bridge (Fig. 3). This structure is only slightly more stable ($\Delta\Delta H = 14.2\,\text{kJ mol}^{-1}$) than the corresponding geometry having the barbiturate double bond *trans* to the polymethine bridge. There is no indication that this latter structure is held in place via hydrogen bonding to the pentamethine protons but the O–H distance is only 2.15 Å. The connecting single bond has a bond length of 1.442 Å and, according to the procedure introduced by Pauling, this bond has about 20% double bond character. Rotation around this latter bond is restricted and the activation energy for interconversion between the two stable forms is ca. $53\,\text{kJ mol}^{-1}$. It is notable that the molecule is out-of-plane by ca. 10° in both stable geometric forms.

Isomerization can also be considered at the first and/or second double bonds in the polymethine bridge. This requires a much larger structural change. The two isomers (Fig. 4) are considerably less stable than the proposed ground-state structure and the activation energies for isomerisation of the ground state are 159 and $218\,\text{kJ mol}^{-1}$, respectively, for rotation around the first and second double bonds in the pentamethine unit. In principle, isomerisation could take place around the third double bond but, since this gives the same product, this process was ignored.

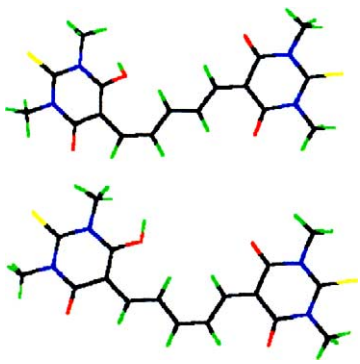

Fig. 4. Computer generated ball and stick representations of the two feasible *cis* isomers of OXON.

Of these various processes, isomerisation at the barbiturate unit is the easiest and the most likely to compete with radiative and nonradiative deactivation of the first-excited singlet state. A set of calculations was made in order to obtain an optimised structure for the hypothetical transition state for interconversion between the two stable isomers. This species has the barbiturate double bond held at an angle of 105° to the plane of the first double bond in the pentamethine unit. Calculations were then made in order to measure the heat of formation as a function of torsion angle. From this, we get the activation energy of $52.7\,\text{kJ mol}^{-1}$.

3.3. Photophysical properties of OXON in various solvents

3.3.1. Linear alkanol solvents

From previous studies it is known that the principal route for deactivation of the first-excited singlet state of OXO involves isomerisation of one of the trimethine double bonds [13]. This process necessitates large-scale torsional motion and will involve frictional forces with adjacent solvent molecules. In an attempt to assess the likelihood of such interactions being important in the photophysical properties of OXON, absorption and emission spectra were recorded in a series of alkanols of varying viscosity. A typical absorption and fluorescence spectral profile recorded for OXON in dilute ethanol is depicted in Fig. 5. The absorption maximum is red-shifted by ca. 100 nm with respect to OXO, due to the more extended polymethine backbone. The fluorescence excitation spectrum gave a satisfactory match to the absorption spectrum over the entire spectral range. The relatively small Stokes' shift ($515 \pm 25\,\text{cm}^{-1}$) is typical of a bis-oxonol and indicates the absence of major geometric changes upon promotion to the first-excited singlet state. It is notable that the Stokes' shift value is ap-

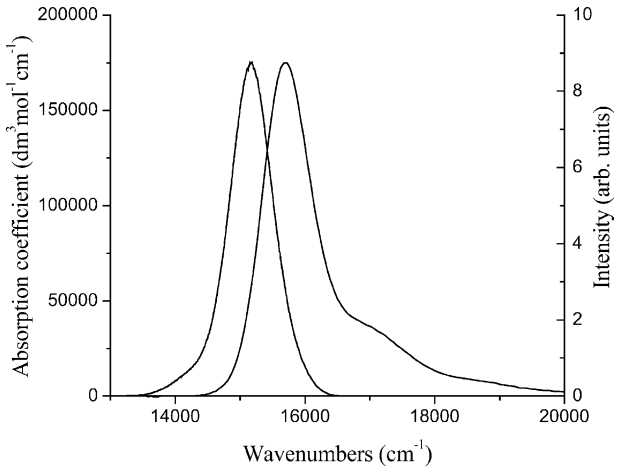

Fig. 5. Absorption and fluorescence spectra recorded for OXON in dilute ethanol at 20 °C.

Table 1
Parameters measured for OXON in linear alkanol solvents at 20 °C

Solvent	ϕ_f[a]	τ_s (ns)[b]	k_f (10^8) s^{-1}	Viscosity (cP)[c]
Methanol	0.38	2.43	1.56	0.580
Ethanol	0.35	2.25	1.55	1.160
Propan-1-ol	0.38	2.41	1.58	2.092
Butan-1-ol	0.37	2.37	1.56	2.849
Pentan-1-ol	0.37	2.38	1.55	4.000
Hexan-1-ol	0.38	2.42	1.57	4.926
Heptanol	0.36	2.34	1.54	6.579
Octanol	0.35	2.26	1.55	8.197
Nonanol	0.38	2.45	1.55	10.417
Decanol	0.34	2.20	1.54	14.286

[a] ±5%.
[b] ±0.08 ns.
[c] Values taken from Ref. [15].

preciably smaller (~20%) than that found for OXO in dilute ethanol.

The fluorescence quantum yield (ϕ_f) of OXON was measured in dilute ethanol relative to free-base meso-tetraphenylporphyrin and was found to be 0.35 ± 0.03. The fluorescence lifetime (τ_s) measured by single photon counting methods was found to be 2.25 ± 0.05 ns and essentially independent of the concentration of oxygen. The radiative rate constant (k_f) was calculated to be $2.6 \pm 0.2 \times 10^8\ s^{-1}$ using the Strickler–Berg expression [14]:

$$k_f = 2.88 \times 10^{-9}\, n^2 \frac{\int F(\nu)\mathrm{d}\nu}{\int (F(\nu)\mathrm{d}\nu/\nu^3)\mathrm{d}\nu} \int \frac{\varepsilon(\nu)}{\nu}\mathrm{d}\nu$$

where $F(\nu)$ is the fluorescence intensity at wavenumber ν and n is the solvent refractive index. There is good agreement between the calculated value and that measured ($k_f = \phi_f/\tau_s$) by emission spectroscopy. In linear alkanol solvents of varying viscosity, ϕ_f, τ_s and k_f values remain essentially independent of bulk viscosity (Table 1). These results are in stark contrast to those collected for related cyanine dyes, for which a major deactivation pathway of the excited state involves isomerisation around a double bond. It would, therefore, seem that isomerisation from the first-excited singlet state of OXON is negligible.

3.4. Measurement of the dipole moment

The variation of the Stokes shift with solvent polarity for protic and aprotic solvents was analysed in terms of the Lippert–Mataga expression [16] in an effort to determine the change in dipole moment between the ground and first-excited singlet states.

$$\Delta\nu = \nu_{abs} - \nu_{flu} = 2\left[\frac{(\mu_{ex} - \mu_{gs})^2}{\varepsilon_0 hca^3}\right] \cdot \int(\varepsilon)$$

$$\int(\varepsilon) = \left[\frac{\varepsilon - 1}{2\varepsilon + 1}\frac{n^2 - 1}{2n^2 + 1}\right]$$

In this expression, ν_{abs} and ν_{flu} are the absorption and fluorescence maxima (in cm^{-1}) while μ_{ex} and μ_{gs} are the dipole moments for the first-excited singlet state and the ground state, respectively. The term '*a*' in the denominator relates to the radius of a spherical cavity in which the molecule resides and that is provided by the dielectric continuum. For OXON, the value of *a* was taken to be 4.8 Å, this being set by the dimensions of the molecule calculated from molecular mechanics studies. The solvent polarity function contains contributions from both the static dielectric constant (ε) and the refractive index (n). Dilute solutions were used in all experiments and the slit-widths of the fluorescence spectrometer were set to a minimum value. The accuracy in peak locations is ca. ±10 cm^{-1} (Fig. 6).

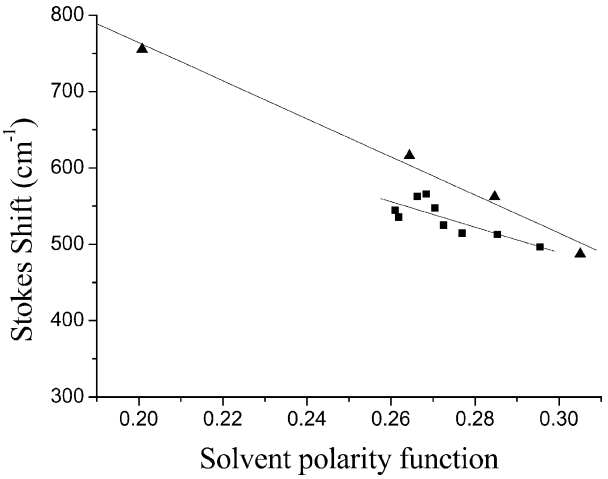

Fig. 6. Effect of solvent polarity, expressed in terms of the polarity function on the Stokes' shift measured for OXON in linear alkanols (■) and aprotic solvents (▲) at 20 °C. The solid line drawn through the data points is a non-linear, least-squares fit to the Lippert–Mataga expression.

Analysis of the solvent polarity effect using the Lippert–Mataga equation afforded a change in dipole moment for OXON of 8.9 ± 0.9 ($2.9 \pm 0.3 \times 10^{-29}$ cm) and 10.9 ± 1.0 D ($3.6 \pm 0.3 \times 10^{-29}$ cm) for protic and aprotic solvents, respectively. Somewhat unusually, the results indicate that the first-excited state is less polar than the corresponding ground state. The fact that results obtained for protic and non-protic solvents fall on separate, but almost parallel lines, is taken as an indication that the former compounds hydrogen bond to OXON. The ground-state dipole moment calculated by semi-empirical AM1 methods for the most stable all-*trans* isomer was found to be 8.18 D (2.73×10^{-29} cm) while that of the first excited singlet state was calculated to be 5.20 D (1.73×10^{-29} cm). Thus, the quantum chemical calculations are in line with experimental observations but the magnitude of the change in dipole moment is inconsistent between theory and experiment. Most likely this problem arises from the uncertainty in finding a suitable value for the radius *a*.

3.5. Activation parameters

The temperature dependence for the rate of decay of the first-excited singlet state of OXON in dilute ethanol

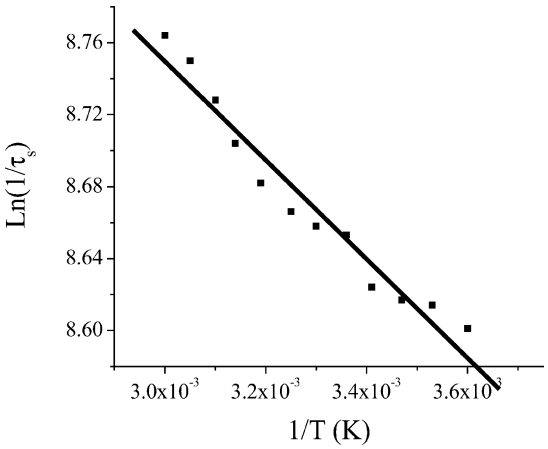

Fig. 7. Arrhenius plot for the temperature dependence of the rate of decay of the first-excited singlet state of OXON in dilute ethanol solution.

($k = 1/\tau_s$) was measured over the range 278–330 K. There is only a very slight temperature effect (Fig. 7) that corresponds to an activation energy (E_a) of 2.3 ± 0.3 kJ mol^{-1}; the corresponding value for OXO is 15.4 kJ mol^{-1}. In fact, the first-excited singlet state of OXON is virtually activationless. This finding, which supports the absence of a significant viscosity effect, indicates that the excited state is resistant to isomerization.

3.6. Quantum chemical studies

For light-induced isomerization to take place it is necessary that the relevant excited state involves the HOMO and LUMO most affected by isomerization. Looking at the MO's associated with the first two excited-singlet states, this seems not to be the case. In part, this is because the molecule seems not to be planar in the ground state. If we assume that isomerization most likely takes place at the barbiturate ring (the one having the hydroxyl group!) then we have to identify the excited state that most affects this subunit. It appears that the first available HOMO has sufficient electron density on the relevant portion of the molecule to be effective at promoting rotation of the barbiturate group. However, the LUMO has the electron density essentially concentrated on the other end of the molecule, especially the carbonyl groups, whilst LUMO-1 and LUMO-2 have the majority of the electron density localised on the carbonyl group of the first barbiturate unit. The most relevant MO to act as acceptor for promoting rotation of the barbiturate ring is LUMO-5. Unfortunately, this MO lies at relatively high energy and is not involved in the lowest-energy, excited singlet states. On this basis, it seems unlikely that light-induced isomerization will make a serious contribution to deactivation of the first excited-singlet state.

3.7. Ion transport properties of OXON

The ability of OXON to act as membrane-bound ion transport carrier was determined by monitoring migration of potassium picrate through 1-decanol supported on a porous, plastic membrane. For comparison, the K^+ ion binding crown ether DB18C6 was also tested under identical conditions. With OXON, the flux for passage of K^+ ions was modest but definitely higher than for control experiments made without carrier. Illumination ($\lambda > 500$ nm) had no effect on the flux. The fact that absorption spectra recorded for OXON in methanol did not change noticeably upon titration with $KClO_4$ indicates that binding between the dye and potassium ion is weak. Comparison experiments performed using DB18C6, which is known to strongly bind K^+ ions but to have a poor releasing affinity (Table 2), gave an average flux ca. 1.7 times higher than found for OXON.

Table 2
Calculated transport properties of OXON

Source: phase/membrane/receiver	Flux (mol s^{-1} m^{-2}) $\times$ 10^7
Kpic (1 mM)/OXON/H_2O[a]	5.01
Kpic (1 mM)/OXON/H_2O[b]	4.72
Kpic (1 mM)/DB18C6/cit (1 M)	8.66
Kpic (1 mM)/DB18C6/cit (0.5 M)	6.98
Kpic (1 mM)/decanol/H_2O	3.20

pic: picrate, cit: citrate.
[a] In dark.
[b] In presence of light.

3.8. Electronic energy transfer

Prior work has identified OXON as a viable candidate for measuring membrane potentials by way of resonance energy transfer. We have already shown that OXON disperses well in artificial membranes and a separate set of experiments showed that this dye is an excellent acceptor for singlet energy transfer from Merocyanine 540 (MC) in fluid solution. Thus, a solution of MC in ethanol was prepared such that the absorbance at 510 nm was 0.10. Fluorescence from the dye could be detected readily at 570 nm. Progressive addition of OXON to this solution resulted in the stepwise extinction of fluorescence from MC and the appearance of fluorescence characteristic of OXON. It should be noted that OXON absorbs only very weakly at 510 nm. The appearance of fluorescence from OXON under these conditions is consistent with Förster-type singlet energy transfer from MC to OXON. The Förster spectral overlap integral for dipole–dipole energy transfer was calculated to be 1.35×10^{-15} mmol^{-1} cm^6 in dilute ethanol solution. Taking this value in conjunction with the assumption of random orientation between the relevant transition dipoles, the critical distance for Förster-type energy transfer from MC to OXON was calculated to be 23 Å. This value corresponds to quite efficient energy transfer since the excited singlet state lifetime of MC is only 240 ps under these conditions. Indeed, the measured bimolecular rate constant for energy transfer in ethanol is 9.5×10^9 dm^3 mol^{-1} s^{-1}.

3.9. Indirect measurement of membrane potential and fluidity

The fact that the photophysical properties of OXON are essentially independent of temperature and viscosity makes for an interesting fluorescence probe by which to measure changes in membrane fluidity and/or potential. In order to record such information it is necessary to use OXON in conjunction with a second fluorophore whose photophysical properties are very sensitive to changes in the local environment. Electronic energy transfer to or from OXON could then be used as the signal output. Merocyanine dyes, which respond well to changes in viscosity, could be used as energy donors while kryptocyanines should make suitable energy acceptors. The advantage of using OXON as an indirect probe in such systems is that donors of inferior fluorescence properties could be used while the difficulties associated with direct excitation of kryptocyanine dyes are circumvented.

4. Conclusion

It has been shown that the photophysical properties of OXON are only slightly dependent on temperature and solvent polarity and essentially insensitive to changes in local viscosity. There is no indication that the first-excited singlet state is susceptible to large-scale torsional motion. Such behaviour is in marked contrast to all other polymethine-based dyes that we have examined. The special properties associated with OXON are believed to arise from the fact that the lowest-energy transitions do not involve the HOMO centred on the molecular fragment most likely to isomerise. This is a consequence of the pentamethine bridge and it is notable that all our earlier studies used smaller bridges. More detailed MO calculations are in progress aimed at better clarifying the orbital picture for the first-excited singlet state.

Acknowledgements

We thank the University of Newcastle, the Procter & Gamble Company and the EPSRC (GR/R23305/01) for financial support of this work. Mr. Alex Bunn is acknowledged for making the preliminary measurements on singlet energy transfer in this system.

References

[1] (a) D.L. Taylor, A.S. Waggoner, R.F. Murphy, F. Lanni, R.R. Birge, in: A.R. Liss (Ed.), Applications of Fluorescence in the Biomedical Sciences, New York, 1986.;
(b) M. Kawakami, K. Koya, T. Ukai, N. Tatsuta, A. Ikegawa, K. Ogawa, T. Shishido, L. Bo Chen, J. Med. Chem. 41 (1998) 130;
(c) A. Mishra, R.K. Behera, P.K. Behera, B.K. Mishra, B.G. Behera, Chem. Rev. 100 (2000) 1973;
(d) S. Bhargava, K. Licha, T. Knaute, B. Ebert, A. Becker, C. Grötzinger, C. Hessenius, B. Wiedenmann, J. Schneider-Mergener, R. Volkmer-Engert, J. Mol. Recognit. 15 (3) (2002) 145.
[2] A. Holoubek, J. Vee, M. Opekarová, K. Sigler, Biochim. Biophys. Acta—Biomembranes 1609 (1) (2003) 71.
[3] (a) K. Venema, R. Gibrat, J.-P. Grouzis, C. Grignon, Biochim. Biophys. Acta—Biomembranes 1146 (1) (1993) 87;
(b) M.A. Haidekker, T. Brady, K. Wen, C. Okada, H.Y. Stevens, J.M. Snell, J.A. Frangos, E.A. Theodorakis, Bioorg. Med. Chem. 10 (11) (2002) 3627;
(c) Y. Onganer, E.L. Quitevis, Biochim. Biophys. Acta—Biomembranes 1192 (1) (1994) 27.
[4] (a) A.C. Benniston, K.S. Gulliya, A. Harriman, J. Chem. Soc., Faraday Trans. 93 (1997) 2491;
(b) A.C. Benniston, A. Harriman, C. McAvoy, J. Chem. Soc., Faraday Trans. 93 (1997) 3653;
(c) A.C. Benniston, A. Harriman, J. Chem. Soc., Faraday Trans. 94 (1998) 1841.
[5] K. Nakshima, T. Ando, T. Nakamizo, S. Akiyama, Chem. Pharm. Bull. 33 (1985) 5380.
[6] F.C. Mohr, C. Fewtrell, J. Immun. 138 (1987) 1564.
[7] A.C. Benniston, A. Harriman, K.S. Gulliya, J. Chem. Soc., Faraday Trans. 90 (1994) 953.
[8] (a) J.R. Lakowicz, G. Piszczek, J.S. Kang, Anal. Biochem. 288 (2001) 62;
(b) M.A. Kessler, O.S. Wolfbeis, Anal. Biochem. 200 (1992) 254.
[9] A. Grinvald, R.D. Frostig, E. Leike, R. Hildesheim, PCT Int. Appl. (2001) 154.
[10] Y. Kuchi, Y. Sakamoto, K. Sawada, J. Chem. Soc., Faraday Trans. 94 (1998) 105.
[11] A. Harriman, R. Hosie, J. Photochem. 15 (1981) 163.
[12] A.C. Benniston, A. Harriman, J. Chem. Soc., Faraday Trans. 90 (1994) 2627.
[13] J. Davila, A. Harriman, K.S. Gulliya, Photochem. Photobiol. 53 (1991) 1.
[14] S.J. Strickler, R.A. Berg, J. Chem. Phys. 37 (1962) 814.
[15] S.L. Murov, Handbook of Photochemistry, Marcel-Dekker, New York, 1973.
[16] (a) N. Mataga, Y. Kaifu, M. Koizumi, Bull. Chim. Soc. Jpn. 28 (1955) 690;
(b) E. Lippert, Z. Naturforsch, A: Astrophys. Phys. Phys. Chem. 10 (1955) 541.